Articles

Discovery and Biological Evaluation of a New Family of Potent Inhibitors of the Dual Specificity Protein Phosphatase Cdc25

John S. Lazo,*,† Diana C. Aslan,‡ Eileen C. Southwick,† Kathleen A. Cooley,† Alexander P. Ducruet,† Beomjun Joo,‡ Andreas Vogt,† and Peter Wipf‡

Departments of Pharmacology and Chemistry, University of Pittsburgh, Pittsburgh, Pennsylvania 15260

Received May 8, 2001

The Cdc25 dual specificity phosphatases have central roles in coordinating cellular signaling processes and cell proliferation, but potent and selective inhibitors are lacking. We experimentally examined the 1990 compound National Cancer Institute Diversity Set and then computationally selected from their 140 000 compound repository 30 quinolinediones of which 8 had in vitro mean inhibitory concentrations <1 μM. The most potent was 6-chloro-7-(2-morpholin-4-ylethylamino)quinoline-5,8-dione (NSC 663284), which was 20- and 450-fold more selective against $Cdc25B_2$ as compared with VHR or PTP1B phosphatases, respectively. NSC 663284 exhibited mixed competitive kinetics against Cdc25A, $Cdc25B_2$, and Cdc25C with K_i values of 29, 95, and 89 nM, respectively. As compared with NSC 663284, the regioisomer 7-chloro-6-(2-morpholin-4-ylethylamino)quinoline-5,8-dione was 3-fold less active against $Cdc25B_2$ in vitro and less potent as a growth inhibitor of human breast cancer cells. Computational electrostatic potential mapping suggested the need for an electron-deficient 7-position for maximal inhibitor activity. Using a chemical complementation assay, we found that NSC 663284 blocked cellular Erk dephosphorylation caused by ectopic Cdc25A expression.

Introduction

Reversible protein phosphorylation is a ubiquitous intracellular process required for mammalian cell communication and growth. Determined by the dynamic balance between protein kinases and phosphatases, serine, threonine, or tyrosine phosphorylation can affect catalytic activity or promote protein−protein interactions that influence subcellular location and functionality. Small molecule inhibitors have provided valuable tools to decode the role of kinases and phosphatases participating in specific cellular signaling pathways, because they are generally reversible and readily enter cells. Natural product inhibitors of serine/threonine protein phosphatases, such as okadaic acid and calyculin A, have been extremely valuable reagents to probe serine/threonine phosphatase function; there is however an absence of potent and selective inhibitors for the other major mammalian phosphatase class, namely, the protein tyrosine phosphatases (PTPase), which includes the dual specificity protein phosphatase (DSPase) subfamily. The PTPases are defined by the active site signature sequence motif HCX_5R, where H is a highly conserved histidine residue, C is the catalytic cysteine, the five X residues form a loop in which all of the amide nitrogens hydrogen-bond to the phosphate of the substrate, and R is a highly conserved arginine that hydrogen bonds to the phosphorylated amino acid of the substrate.[1] While the DSPases retain the conserved HCX_5R motif, they are unique in their ability to hydrolyze both phosphoserine/threonine and phosphotyrosine residues on the same protein substrate.[1] Important members of the DSPase family are the Cdc25 phosphatases, which control cell cycle progression by activating cyclin-dependent kinases (Cdk)[2] and participate in Raf-1-mediated cell signaling.[3]

Three Cdc25 homologues exist in humans: Cdc25A, Cdc25B, and Cdc25C.[2,4−6] Cdc25A and B have oncogenic properties,[7] are transcriptional targets of the c-*myc* oncogene,[8] and are overexpressed in many human tumors.[9,10] Both Cdc25B and Cdc25C are thought to be regulators of G2/M transition through their ability to dephosphorylate and activate the Cdk1/cyclin B mitotic kinase complex, which is required for cell entry into mitosis.[2,11] Cdc25A is likely to be important for G1/S phase transition and in preserving genomic integrity,[12−14] although Cdc25A may also have some role in the initiation of mitosis.[14] Cdc25A is rapidly degraded in response to DNA damage, which impairs the G1/S transition.[15] Cdc25A may also have other cellular roles as it has been shown to regulate the tyrosine phosphorylation status and kinase activity of Raf-1, which has a central role in the mitogen-activated kinase signal transduction pathway.[3]

Although two crystal structures have been published for the Cdc25 catalytic domain,[16,17] none expose the nature of interactions with small molecule inhibitors. Moreover, the protein substrate may initiate key conformational changes and provide an important catalytic acid.[18,19] Thus, rational design parameters for potential inhibitors are lacking. The current work was initiated

* Corresponding author telephone: (412)648-9319; fax: (412)648-2229; e-mail: lazo@pitt.edu.
† Department of Pharmacology.
‡ Department of Chemistry.

10.1021/jm0102046 CCC: $20.00
Published on Web 10/18/2001

Table 1. Chemical Structures of Quinolinedione Cdc25 Inhibitors and In *Vitro* Activity against Recombinant Human $Cdc25B_2$, VHR, or PTP1B[b]

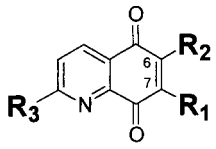

NSC	R_1	R_2	R_3	IC_{50} (μM) Cdc25	VHR	PTP1B
668394	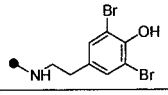	H	H	0.64 ± 0.13	8.5[a]	8.0[a]
663284	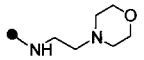	Cl	H	0.21 ± 0.08	4.0 ± 0.1	> 100
45384	NH	OMe	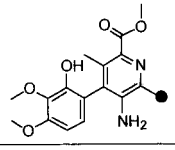	0.37 ± 0.08	5.1 ± 0.1	8.7 ± 0.3
677948	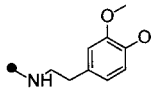	H	H	0.45 ± 0.02	17 ± 0.5	> 100
677949	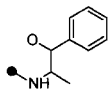	H	H	0.51 ± 0.01	16 ± 2.0	>100
677945	H	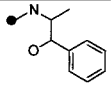	H	0.67 ± 0.04	>10	>10
663282	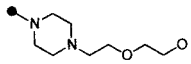	Cl	H	0.90[a]	>10	>10
662383	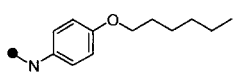	Cl	H	0.93[a]	>10	>10

[a] Single determination. [b] IC_{50} values were from 3 or more determinations with SEM indicated.

based on the belief that selective Cdc25 inhibitors could be obtained by using a general and unbiased approach to evaluate a chemically diverse compound library. Thus, we probed a small subset of the National Cancer Institute's (NCI) 140 000 compound library for a potential inhibitory pharmacophore and used this information to identify a pharmacophore yielding the most potent and selective inhibitor of Cdc25 reported to date. This compound had marked antiproliferative activity against human tumor cells and blocked the biochemical actions of ectopic Cdc25A expression.

Results

Quinolinediones from the NCI Compound Library Inhibited Human Cdc25. Initially, we examined the 1990 compounds comprising the NCI Diversity Set, which was designed to be representative of the 140 000 NCI compound repository. Members of the Diversity Set have been evaluated by the NCI for growth inhibition against the NCI 60 Tumor Cell Panel, and these data are publicly available at http//www.dtp.nci.nih.gov/. We examined the Diversity Set for in vitro inhibition of recombinant full-length human $Cdc25B_2$ and found 24 compounds that caused >80% inhibition at 10 μM. Upon reevaluation, 5 of the 24 compounds had IC_{50} values <1 μM; the most potent $Cdc25B_2$ inhibitor was the quinolinedione NSC 668394, which had an IC_{50} of 640 ± 130 nM against $Cdc25B_2$ and had ≥8-fold preference for $Cdc25B_2$ as compared to the DSPase VHR or the PTPase PTP1B (Table 1). Moreover, the mean IC_{50} for growth inhibition by NSC 668394 was 2.1 ± 2.0 μM when assayed in the NCI 60 Tumor Cell Panel (see http://www.dtp.nci.nih.gov/). NSC 668394 was the sole quinolinedione in the Diversity Set. The importance of the 5,8-dione pharmacophore for Cdc25 inhibition was emphasized by the lack of significant anti-phosphatase activity at 10 μM with any of the other 118 quinoline structures evaluated in the Diversity Set. To test the hypothesis that the quinolinedione pharmacophore was important for Cdc25 inhibitory activity, Jill Johnson (NCI, Developmental Therapeutics Program, Rockville, MD) computationally identified 30 additional quinolinediones in the NCI Compound Repository, and we examined them experimentally for anti-phosphatase activity. When tested, all of these compounds had in vitro IC_{50} values <40 μM for $Cdc25B_2$, and seven had IC_{50} values <1 μM. The mean IC_{50} value was 5.4 ± 1.5 μM. Six of the seven most active compounds were

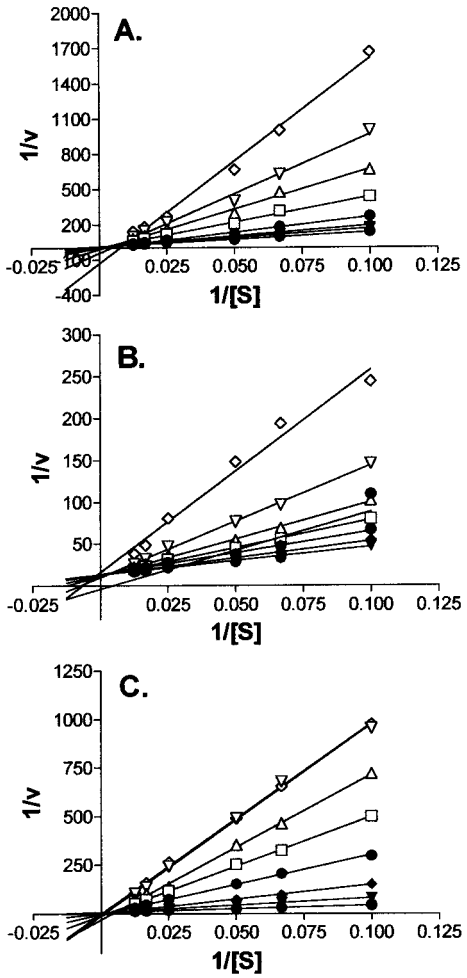

Figure 1. Lineweaver−Burk plots for NSC 663284 inhibition of Cdc25 isoforms. (A) Cdc25A. Concentrations of NSC 663284 are ▼, 15; ◆, 25; ●, 50; □, 100; △, 150; ▽, 200; ◇, 300 nM. (B) $Cdc25B_2$, ▼, 25; ◆, 50; ●, 100; □, 150; △, 200; ▽, 300; ◇, 500 nM. (C) Cdc25C. ▼, 25; ◆, 50; ●, 100; □, 150; △, 200; ▽, 300; ◇, 500 nM.

7-substituted quinolinediones, with the most potent (NSC 663284) having an IC_{50} value of 206 ± 75 nM (Table 1). All of the submicromolar inhibitors displayed a strong preference for $Cdc25B_2$ as compared with VHR or PTP1B. For example, with NSC 663284, the relative IC_{50} values for $Cdc25B_2$ were 20- and 450-fold lower than for VHR or PTP1B, respectively.

We examined further the kinetics and relative sensitivity of each of the full-length human Cdc25 isoforms to NSC 663284. For all three Cdc25 isoforms, NSC 663284 inhibition kinetics fit best to a partial mixed competitive model, which may reflect the potential for interactions at the two anionic binding sites as observed in the crystal structure of Cdc25B[17] (Figure 1). The calculated K_i values for Cdc25A, Cdc25B, and Cdc25C were 29 ± 7, 95 ± 14, and 89 ± 18 nM (n = 4−6, ± SEM), respectively, suggesting that NSC 663284 had 3-fold selectivity toward Cdc25A as compared with either Cdc25B or Cdc25C.

Analogue Analyses Revealed the Importance of the C-7 Substitution for Potent Cdc25 Inhibition. To interrogate further the quinolinedione pharmacophore, we resynthesized NSC 663284, DA3003-1, and synthesized the regioisomer of NSC 663284, namely,

Table 2. Structures and Activity of Synthesized Heteroarenedione Analogues[b]

Name	Structure	IC_{50} (μM)		
		$Cdc25B_2$	VHR	PTP1B
DA3003-2	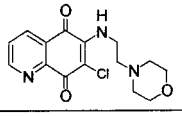	0.82 ± 0.08	>10	>10
DA276	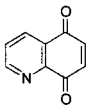	3.0 ± 1.4	>10	>10
DA3002	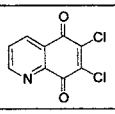	4.6 ± 1.0	>10	>10
DA3100	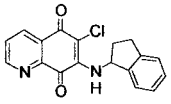	0.30 ± 0.03	ND	ND
DA3018	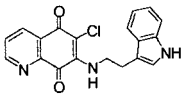	5.1 ± 0.6	>10	>10
DA3020	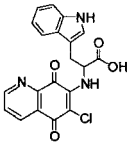	16 ± 4	>10	>10
DA295	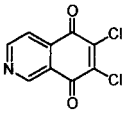	1.5 ± 0.7	>10	>10
DA3044	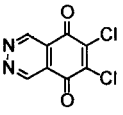	8.9 ± 5.0	>10	>10
DA3045	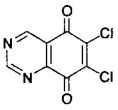	4.8 ± 2.8	>10	>10
DA296	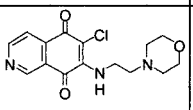	0.59 ± 0.18	>10	>10
DA3049	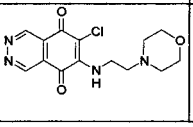	0.43 ± 0.03	1.1[a]	9.8[a]

[a] Single determination. [b] IC_{50} values were from 3 or more determinations with SEM indicated. ND = not determined.

DA3003-2, as well as several other analogues. A comparative study with the minimal quinolinedione, isoquinolinedione, phthalazinedione, and quinazolinedione (namely, DA276, DA3002, DA295, DA3044, and DA3045) revealed that a heterocyclic quinone pharmacophore alone was insufficient for potent Cdc25 inhibition (Table 2). NSC 663284 had identical inhibitory properties as compared to DA3003-1 against Cdc25A, Cdc25B, and Cdc25C as well as HPLC and spectral profiles. Thus, we used NSC 663284 for most of the subsequent biological studies because of the much greater quantities

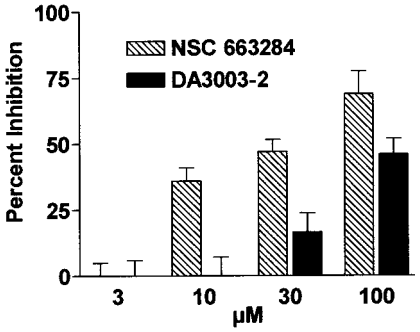

Figure 2. Growth inhibition of NSC 663284 and DA3003-2. Cells were treated for 3 h with NSC 663284 (hatched bars) or the regioisomeric DA3003-2 (black bars), and cell growth was determined 48 h later as described in the Experimental Section.

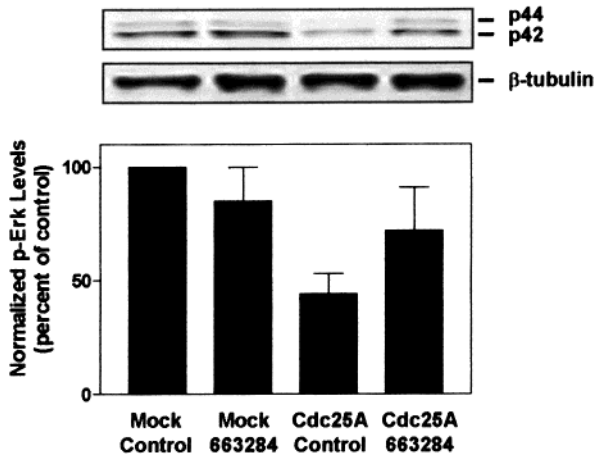

Figure 3. Reduction of phospho-Erk levels by Cdc25A overexpression and inhibition of Cdc25A activity by NSC 663284. (Upper Panel) Western blot of phospho-Erk levels after mock transfection (lanes 1 and 2) or wild-type human Cdc25A transfection (lanes 3 and 4). Cells were treated for 1 h with vehicle (lanes 1 and 3) or 10 μM NSC 663284 (lanes 2 and 4). (Middle Panel) β-tubulin was used as a loading control. (Lower Panel) Quantification of the phospho-Erk levels in cells after treatment with NSC 663284. $n = 4$; bars = SEM. Only Cdc25A control was less than mock control ($p < 0.05$, Student's t-test).

available to us. Addition of the 2-morpholin-4-ylethylamino moiety at the 7-position clearly enhanced inhibitory activity against Cdc25B as indicated by comparing the IC_{50} values of DA3049 with DA3044, of DA296 with DA295, or of NSC 663284 with either DA3002 or DA276. Other 7-substituted analogues, such as DA3018 and DA3020, were poor inhibitors of Cdc25B, although DA3100 exhibited significant inhibitory activity indicating that the 2-morpholin-4-ylethylamino moiety was one of at least two unique enhancers. For this limited series, the quinolinedione pharmacophore provided a superior scaffold as compared to the other heterocycles. Thus, the quinoline analogue NSC 663284 was a more potent inhibitor than either the isoquinoline analogue DA296 or the phthalazine analogue DA3049. The 7-substituted quinolinedione NSC 663284, which contained the 2-morpholin-4-ylethylamino moiety at the 7-position, was also approximately 3-fold better as an inhibitor of $Cdc25B_2$ than its regioisomer DA3003-2 and was the most potent inhibitor of all compounds tested.

NSC 663284 Blocked Cell Proliferation and the Actions of Cellular Cdc25A. NSC 663284 had a mean IC_{50} value in the NCI 60 Cell Human Tumor Panel of 1.5 ± 0.6 μM when cells were treated for 48 h. Most sensitive were human breast cancer MDA-MB-435 and MDA-N cells, which had IC_{50} values of 0.2 μM. We observed an IC_{50} for growth inhibition of 1.7 μM with continuous 48-h NSC 663284 treatment of human breast MCF-7 cells in culture (data not shown). Even after only a 3-h exposure to NSC 663284, we observed an IC_{50} for growth inhibition of $\sim$35 μM with MCF-7 cells (Figure 2). Consistent with in vitro Cdc25 inhibition, the IC_{50} for growth inhibition after a 3-h exposure to NSC 663284 was 3-fold lower than that seen with the 6-regioisomer DA3003-2 (Figure 2). To probe for inhibition of cellular Cdc25 activity, we used a recently described chemical complementation assay,[20] which revealed the ability of a small molecule to complement or reverse a biochemical effect caused by ectopic Cdc25A expression. The advantage of this assay for studying small molecules that also may affect cell cycle progression is the requirement for only a brief exposure of an asynchronous cell population to an agent. Cdc25A has been implicated in controlling the phosphorylation status of Raf-1, which is a proximal effector of the mitogen-activated protein kinase (Erk1/2) pathway.[3] Thus, transient expression of full-length Cdc25A in HeLa cells resulted in a >50% decrease in Erk phosphorylation (Figure 3). Treatment of mock (no Cdc25) transfected cells with 10 μM NSC 663284 caused no significant increase in Erk phosphorylation while exposure of Cdc25A transfected cells for 1 h to 10 μM NSC 663284 reversed the depression of Erk phosphorylation caused by Cdc25A transfection and returned phospho-Erk to constitutive levels (Figure 3). These results support the hypothesis that NSC 663284 blocked the biological effects of Cdc25A within cells.

The substitution with amino groups at 6- and 7-positions, respectively, of the quinone cores of NSC 663284 and DA3003-2 was significant for increasing inhibitory activity. This effect could be due to a polarization of the electron distribution in the quinolinedione, since the decrease in activity of the chlorinated derivative is considerable and the difference in activity between DA3100 and NSC 663284 was much less pronounced. The latter two compounds would be expected to exhibit a closely related electronic polarization of the quinone core. IC_{50} values of NSC 663284, NSC 668394, DA3100, DA296, DA3049, and DA3003-2 vary by a factor of 3, while IC_{50} values for the corresponding dichloro analogues DA3002, DA295, and DA3044 are about an order of magnitude higher. Electron density surfaces encoded with the electrostatic potential obtained by ab initio computation of the core pharmacophore structure demonstrate that, despite significant differences in the position and the number of nitrogen atoms, NSC 663284, DA296, DA3049, and DA3003-2 have closely related, polarized electron distributions (Figure 4). In comparison, the analogous graphs for dichloro analogues DA3002, DA295, and DA3044 show a very different, much less polarized electrostatic potential surface (Figure 5). On the basis of this analysis, it becomes clear that replacing a chloride substituent with an amino group leads to a considerable perturbation of the electron distribution in heteronaphthoquinones and that

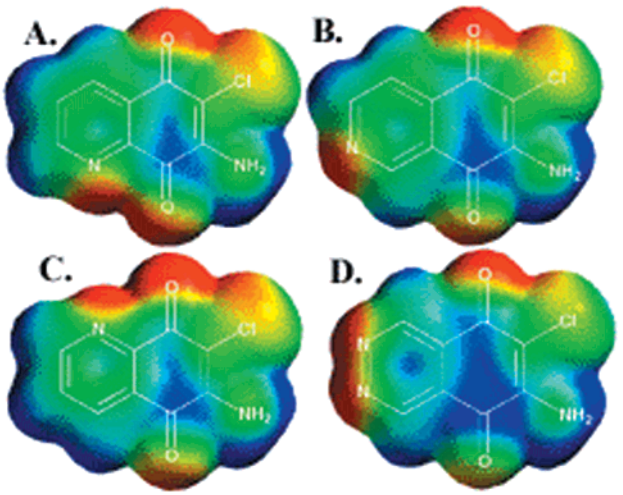

Figure 4. Electrostatic potential-encoded electron density surfaces of the core structures of NSC 663284 (A), DA296 (B), DA3003-2 (C), and DA3049 (D). The surfaces were generated with Spartan 5.1.1 (Wavefunction, Inc.) after ab initio minimization with a 3-21G* basis set. The coloring represents electrostatic potential with red indicating the strongest attraction to a positive point charge and blue indicating the strongest repulsion. The electrostatic potential is the energy of interaction of the positive point charge with the nuclei and electrons of a molecule. It provides a representative measure of overall molecular charge distribution.

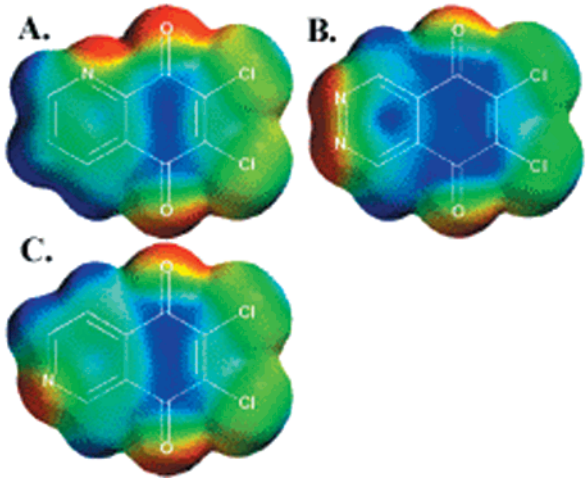

Figure 5. Electrostatic potential-encoded electron density surfaces of less active core structures: DA3002 (A), DA295 (B), and DA3044 (C). The surfaces were generated with Spartan 5.1.1 (Wavefunction, Inc.) after ab initio minimization with a 3-21G* basis set.

this electrostatic effect is likely to provide a better match for the complementary surface in the enzyme binding pocket. The core structure of NSC 663284 could therefore represent a general motif for the electronic configuration that is necessary to achieve selective and potent Cdc25 inhibition.

Discussion

Although there is consensus that DSPases have important roles in controlling cell proliferation and signaling pathways, the absence of potent and selective inhibitors has limited our ability to probe their biological function. For example, until recently the only readily available Cdc25 inhibitor was the broad spectrum PTPase inhibitor sodium orthovanadate. More recently, several small molecule Cdc25 phosphatase inhibitors have been reported such as dysidiolide ($IC_{50} = 9.4\ \mu M$),[21] sulfircin ($IC_{50} = 7.8\ \mu M$),[22] SC-ααδ9 ($IC_{50} = 15\ \mu M$),[23] FY21-αα09 ($IC_{50} = 7\ \mu M$),[24] a cyano-containing cholesteryl derivative ($IC_{50} = 2.2\ \mu M$),[25] and a vitamin K analogue called **5** ($IC_{50} = 3.8\ \mu M$).[26] Of interest to our study was the previous identification of tetrahydroisoquinolines with some inhibitory activity against Cdc25B ($IC_{50} = 15-35$ mM).[27] Most of the above-mentioned agents have not been evaluated for specificity and, with the exception of **5** and SC-ααδ9, none have been shown to inhibit Cdc25 within cells. Moreover, all of these compounds lack the desired potency for exceptional inhibitors.

Our studies illustrate how a subset of compounds selected from a chemical library based on chemical diversity can be used to screen against a predicted end point and yield potent bioactive compounds. The quinoline-5,8-diones have been the focus of previous studies because of their wide spectrum of biological activity including antitumor, antifungal, and antimalarial effects.[28] Despite considerable investigation, their mechanism of action is largely not understood. For quinolinediones, such as streptonigrin and lavendamycin, depletion of NADPH/NADH, uncoupling of oxidative phosphorylation, and/or DNA cleavage has been suggested.[29] Although we cannot formally exclude such mechanisms for the cytotoxic effects of NSC 663284, one advantage of our chemical complementation assay is that it provides one with the ability to examine cellular events after only a relatively brief exposure to an agent. This is especially important for agents that block cell proliferation. Thus, the chemical complementation assay provided experimental evidence that NSC 663284 can block the intracellular actions on the expressed target, namely, Cdc25A. Moreover, the regioisomer that was a superior inhibitor of Cdc25 in vitro was more cytotoxic after a brief cell exposure. Interestingly, we found no significant difference in the cytotoxicity of the two regioisomers when cells were treated continuously with these two regioisomers, suggesting that prolonged exposure may cause other toxic actions. Consistent with this notion is the observation that after prolonged exposure isoquinolinediones are more toxic to cells than their respective quinolinediones[30] even though in our studies the quinolinediones were more potent as in vitro inhibitors of Cdc25 than the corresponding isoquinolinediones (Table 2). Preliminary molecular modeling studies with the available crystal structures for Cdc25B are consistent with the quinolinedione pharmacophore binding in at least one of the Cdc25 anionic binding sites and provide a hypothetical explanation for the regioisomeric preference that can be tested with newer analogues (manuscript in preparation). As shown in the electrostatic potential maps, the nitrogen-substituted carbon of the ene-5,8-dione moiety in these inhibitors is the most electron-deficient center of the quinone substructure. While these computational electrostatic potential mapping studies suggest the need for an electron-deficient 7-position for maximal inhibitor activity, it is evident that the potency of inhibitors was not simply correlated with increasing electrophilicity at this position, which follows the series NSC 663284 < DA3003−2 < DA296 < DA3049. This would be consis-

tent with the notion that the pendant moieties on the 7-position also are important.

We noted some modest selectivity for inhibition of Cdc25A as compared with Cdc25B and Cdc25C. Although there is no available crystal structure of a ligand with any Cdc25 isoform, structural differences in the catalytic region of Cdc25A and Cdc25B have been noted.[16,17] Moreover, protein substrate preferences have been reported with Cdc25A and Cdc25C, which reflect not only residues within the catalytic domain but others as yet undefined outside of the catalytic domain.[17,18] Our results suggest that it may be feasible to identify small molecules with significant specificity for individual Cdc25 isoforms. These would be valuable reagents as there continues to be controversy about the precise cellular actions of some of the isoforms. We suggest that quinolinediones have a rich potential as a pharmacophore for inhibitors of the DSPase Cdc25 and that they could represent useful biochemical probes as well as possible lead compounds for the design of agents for the treatment of cancer or other diseases.[2,18]

Experimental Section

Library Chemicals. The Diversity Set and selected quinolinediones were the kind gift of Jill Johnson (NCI, National Institutes of Health, Developmental Therapetuics Program, Rockville, MD). The Diversity Set was generated by the NCI from the 140 000 compounds in the NCI Compound Repository based first on the availability of ≥1 g in their Repository, which reduced the total eligible compounds to 71 756. Chem-X (Oxford Molecular Group) was then used to define hydrogen bond acceptor, hydrogen bond donor, positive charge, aromatic, hydrophobic, acid, base, and distance intervals to create a particular finite set of pharmacophores. The default setting of 3-point pharmacophores resulted in almost 10^6 possible pharmacophores. The Chem-X diverse subset generating function was used to determine the acceptable conformations of individual structures and the acceptable pharmacophore for the conformation. The Diversity Set was populated in a comparative iterative manner with a requirement of ≤5 rotatable bonds. Because the selection procedure was order dependent, the order in which the structures were considered was randomized. This procedure resulted in the selection of 1990 compounds; more information about the NCI Diversity Set can be found at http://dtp.nci.nih.gov/.

Synthesis of Compounds. All moisture-sensitive reactions were performed under an atmosphere of dry nitrogen, and all glassware were dried in an oven prior to use. THF and ether were dried by distillation over sodium benzophenone and CH_2Cl_2 was dried by distillation over CaH_2. Unless otherwise stated, all commercially available materials were used without purification. IR spectra were recorded neat using NaCl cells. NMR spectra were obtained at 300 MHz/75 MHz (^{1}H/^{13}C NMR) in $CDCl_3$ unless noted otherwise. High- and low-resolution masses were determined by introduction with a direct insertion probe into a VG-70-70 HF spectrometer operating in the electron ionization mode. The purity of synthetic DA3002, DA296, DA3003-1, DA3003-2, and DA3049 was ascertained by HRMS and HPLC analyses in two different mobile phases to be at least 94%, in most cases >99% (see Supporting Information for details of the analyses).

DA276 (Quinoline-5,8-dione). Prepared in 56% yield from quinoline-8-ol according to literature procedures:[31] ^{1}H NMR: δ 9.06 (dd, 1 H, J = 4.6, 1.6 Hz), 8.43 (dd, 1 H, J = 7.8, 1.6 Hz), 7.72 (dd, 1 H, J = 7.8, 4.6 Hz), 7.16 (d, 1 H, J = 10.0 Hz), 7.07(d, 1 H, J = 10.0 Hz). HRMS (EI) m/z: calcd for $C_9H_5NO_2$, 159.0320; found: 159.0321.

DA295 (6,7-Dichloroisoquinoline-5,8-dione). Prepared according to literature procedures:[30] ^{1}H NMR (MeOH-d_4, δ): 9.33 (s, 1 H), 9.08 (d, 1 H, J = 5.1 Hz), 8.08 (d, 1 H, J = 5.1 Hz). ^{13}C NMR (MeOH-d_4, δ): 173.8 (2C), 153.5, 146.7, 141.8, 141.7, 135.7, 123.4, 118.0. MS (EI) m/z (rel intensity): 227 (M^+, 100), 199 (20), 192 (80), 164 (80). HRMS (EI) m/z: calcd for $C_9H_3NO_2Cl_2$, 226.9541; found, 226.9544.

DA296 (6-Chloro-7-(2-morpholin-4-ylethylamino)isoquinoline-5,8-dione). A solution of DA295 (114 mg, 0.500 mmol) and 2-morpholin-4-ylethylamine (65 mg, 0.50 mmol) in 5 mL of THF was treated with triethylamine (0.07 mL, 0.5 mmol) at room temperature. The reaction mixture was stirred for 20 h at room temperature, concentrated under reduced pressure, diluted with ethyl acetate, and washed with water. The organic layer was dried (Na_2SO_4) and concentrated in vacuo. The crude residue was purified by chromatography on SiO_2 (CH_2Cl_2/MeOH, 15:1) to give a 4:1 mixture of DA296 and its regioisomer (110 mg, 69%). The major regioisomer was assigned based on ^{1}H NMR analysis.[32] Separation of isomers by chromatography on SiO_2 (CH_2Cl_2/MeOH, 50:1) or recrystallization from Et_2O/hexanes provided DA296 in ca. 90% purity as a dark red solid: mp 125 °C (dec). IR (neat): 3271, 2958, 2851, 1683, 1640, 1600, 1564, 1113 cm^{-1}. ^{1}H NMR: δ 9.24 (s, 1 H), 9.00 (d, 1 H, J = 5.0 Hz), 7.94 (d, 1 H, J = 5.0 Hz), 7.13 (br, 1 H), 4.02−3.96 (m, 2 H), 3.78−3.75 (m, 4 H), 2.69 (t, 2 H, J = 5.6 Hz), 2.54 (m, 4 H). ^{13}C NMR: δ 179.9, 175.0, 156.3, 154.3, 148.5, 138.2, 123.7, 119.1, 118.2, 67.0 (2C), 56.6, 53.0 (2C), 40.9. MS (EI) m/z (rel intensity): 323 ([M + 2]$^+$, 5), 221 (35), 101 (100). HRMS (EI) m/z: calcd for $C_{15}H_{18}N_3O_3Cl$ (M + 2H), 323.1037; found: 323.1037.

DA3002 (6,7-Dichloroquinoline-5,8-dione). Prepared in 30−40% yield from quinoline-8-ol according to literature procedures:[20] ^{1}H NMR (DMSO-d_6, δ): 9.01 (dd, 1 H, J = 3.8, 1.2 Hz), 8.41 (dd, 1 H, J = 7.3, 1.2 Hz), 7.86 (dd, 1 H, J = 7.3, 3.8 Hz). ^{13}C NMR (DMSO-d_6, δ): 176.0, 174.3, 154.5, 147.1, 143.1, 141.6, 134.9, 128.5, 128.3. MS (EI) m/z (relative intensity): 227 (M^+, 100), 199 (80), 192 (25), 136 (100). HRMS (EI) m/z: calcd for $C_9H_3NO_2Cl_2$, 226.9541; found: 226.9545.

DA3003-1 (NSC 663284, 6-Chloro-7-(2-morpholin-4-ylethylamino)quinoline-5,8-dione) and DA3003-2 (7-Chloro-6-(2-morpholin-4-ylethylamino)quinoline-5,8-dione). A solution of DA3002 (228 mg, 1.00 mmol) and 2-morpholin-4-ylethylamine (130 mg, 1.00 mmol) in 5 mL of THF was treated at room temperature with triethylamine (0.14 mL, 1.0 mmol). The reaction mixture was stirred for 20 h at room temperature, concentrated under reduced pressure, diluted with ethyl acetate, and washed with water. The organic layer was dried (Na_2SO_4) and concentrated in vacuo. The crude residue was purified by chromatography on SiO_2 (CH_2Cl_2/MeOH, 15:1) to give a 2:1 mixture (^{1}H NMR) of DA3003-1 and DA3003-2 (260 mg, 80%). Further separation by chromatography on SiO_2 (CH_2Cl_2/MeOH, 50:1) gave pure DA3003-1 and DA3003-2 as dark red, amorphous solids. The 5,8-quinolinedione regioisomers were assigned based on the known preference for nucleophilic addition at the 7-position in aprotic solvents and the observation that $\Delta\delta$ (H2−H4) of the 6-isomer is higher than that of the 7-isomer in ^{1}H NMR.[32] 5,8-Isoquinolinedione regioisomers were assigned based on the known preference for nucleophilic additions at the 7-position[33] and the apparent trend that $\Delta\delta$ (H1−H4) of the 6-isomer is higher than that of the 7-isomer in ^{1}H NMR.

DA3003-1. IR (neat): 3275, 2958, 2855, 1695, 1636, 1600, 1568, 1109 cm^{-1}. ^{1}H NMR: δ 8.92 (dd, 1 H, J = 4.7, 1.6 Hz), 8.48 (dd, 1 H, J = 7.8, 1.6 Hz), 7.66 (dd, 1 H, J = 7.8, 4.7 Hz), 7.09 (br, 1 H), 4.05−3.95 (m, 2 H), 3.80−3.70 (m, 4 H), 2.70 (t, 2 H, J = 5.7 Hz), 2.65−2.45 (m, 4 H). ^{13}C NMR: δ 179.0, 175.4, 153.4, 146.2, 145.3, 134.6, 129.8, 128.4, 67.0 (2C), 56.7, 53.0 (2C), 40.9. MS (EI) m/z (rel intensity): 323 ([M + 2]$^+$, 7), 210 (25), 100 (100). HRMS (EI) m/z: calcd for $C_{15}H_{18}N_3O_3Cl$ (M + 2H), 323.1037; found: 323.1034. A direct comparison between DA3003-1 and NSC 663284 showed no detectable difference in HPLC profiles, chemical properties, enzyme inhibitory effects, or growth inhibition. Thus, most of the reported cellular and kinetic studies were performed with NSC 663284 because of the limited amount of DA3003-1.

DA3003-2. IR (neat): 3275, 2958, 2851, 1687, 1647, 1600, 1564, 1106 cm^{-1}. ^{1}H NMR: δ 9.02 (dd, 1 H, J = 4.6, 1.6 Hz), 8.36 (dd, 1 H, J = 8.0, 1.6 Hz), 7.59 (dd, 1 H, J = 8.0, 4.6 Hz),

6.98 (br, 1 H), 4.0−3.9 (m, 2 H), 3.8−3.7 (m, 4 H), 2.70 (t, 2 H, $J = 5.4$ Hz), 2.6−2.45 (m, 4 H). ^{13}C NMR: δ 180.3, 175.2, 155.4, 148.6, 144.4, 134.8, 127.0, 126.7, 67.1 (2C), 56.8, 53.1 (2C), 40.8. MS (EI) *m/z* (rel intensity): 323 ([M + 2]$^+$, 40), 285 (8) 267 (10), 100 (100). HRMS (EI) *m/z*: calcd for $C_{15}H_{18}N_3O_3Cl$ (M + 2H), 323.1037; found: 323.1027.

DA3044 (6,7-Dichlorophthalazine-5,8-dione). Prepared according to literature procedures:[33] ^{1}H NMR: δ 9.93 (s, 2 H). MS (EI) *m/z* (rel intensity): 228 (M$^+$, 100), 200 (30). HRMS (EI) *m/z*: calcd for $C_8H_2N_2O_2Cl_2$, 227.9493; found: 227.9492.

DA3045 (6,7-Dichloroquinazoline-5,8-dione). Prepared according to literature procedures:[33] ^{1}H NMR: δ 9.75 (s, 1 H), 9.64 (s 1 H). MS (EI) *m/z* (rel intensity): 228 (M$^+$, 100), 200 (30), 165 (30), 110 (30), 87 (40). HRMS (EI) *m/z*: calcd for $C_8H_2N_2O_2Cl_2$, 227.9493; found: 227.9497.

DA3049 (6-Chloro-7-(2-morpholin-4-ylethylamino)phthalazine-5,8-dione). A solution of DA3044 (67 mg, 0.29 mmol) and 2-morpholin-4-ylethylamine (38 mg, 0.29 mmol) in 5 mL of THF was treated at room temperature with triethylamine (0.04 mL, 0.3 mmol). The reaction mixture was stirred for 2 h at room temperature, concentrated under reduced pressure, diluted with ethyl acetate, and washed with water. The organic layer was dried (Na_2SO_4) and concentrated in vacuo. The crude residue was purified by chromatography on SiO_2 (CH_2Cl_2/MeOH, 15:1) to give pure DA3049 (42 mg, 45%) as a dark red, amorphous sticky solid. IR (neat): 3271, 2958, 2923, 2855, 2808, 1695, 1636, 1556, 1311, 1295, 1113 cm^{-1}. ^{1}H NMR: δ 9.83 (s, 1 H), 9.65 (s, 1 H), 7.18 (br, 1 H), 4.00−3.90 (m, 2 H), 3.75−3.70 (m, 4 H), 2.69 (t, 2 H, $J = 6.0$ Hz), 2.55−2.50 (m, 4 H). ^{13}C NMR: δ 180.5, 174.2, 171.4, 147.2, 145.3, 144.5, 124.8, 123.3, 67.1 (2C), 56.3, 53.0 (2C), 41.0. MS (EI) *m/z* (rel intensity): 324 ([M + 2]$^+$, 10), 286 (12), 256 (8), 235 (12) 100 (100). HRMS (EI) *m/z*: calcd for $C_{14}H_{17}N_4O_3Cl$ (M + 2H), 324.0989; found: 324.0989.

DA3100 (6-Chloro-7-(indan-2-ylamino)quinoline-5,8-dione). According to the procedure described for DA3003-1, DA3100 (192 mg, 59%) was obtained from DA3002 (228 mg, 1.00 mmol) and 1-aminoindane (133 mg, 1.00 mmol) as a dark red, amorphous sticky solid. IR (neat): 3323, 3065, 2939, 2844, 1695, 1640, 1592, 1560, 1315, 721 cm^{-1}. ^{1}H NMR: δ 8.92 (dd, 1 H, $J = 4.6$, 1.4 Hz), 8.49 (dd, 1 H, $J = 7.8$, 1.4 Hz), 7.67 (dd, 1 H, $J = 7.8$, 4.6 Hz), 7.29−7.22 (m, 4 H), 6.40 (br, 1 H), 6.18−6.10 (m, 1 H), 3.13−2.92 (m, 2 H), 2.78−2.72 (m, 1 H), 2.13−2.06 (m, 1 H). ^{13}C NMR: δ 178.8, 175.8, 153.5, 146.0, 144.2, 143.5, 142.4, 134.8, 130.0, 128.8, 128.5, 127.3, 125.2, 124.5, 59.8, 36.3, 20.2. MS (EI) *m/z* (rel intensity): 324 (M$^+$, 30), 287 (15), 220 (15), 205(35), 117 (100). HRMS (EI) *m/z*: calcd for $C_{18}H_{13}N_2O_2Cl$, 324.0666; found: 324.0656.

In Vitro Enzyme Assays. The activities of the GST-fusion Cdc25A, Cdc25B$_2$, Cdc25C, and VHR as well as human recombinant PTP1B were measured using *o*-methyl fluorescein phosphate (Sigma, St. Louis, MO) as substrate and a miniaturized, 96-well microtiter plate assay based on previously described methods.[23] The final incubation mixtures (25 μL) were prepared using a Biomek 2000 laboratory automation workstation (Beckman Coulter, Inc., Fullerton, CA). Fluorescence emission from the product was measured after a 60-min incubation period at ambient temperature with a multiwell plate reader (PerSeptive Biosystems Cytofluor II; Framingham, MA; excitation filter, 485/20; emission filter, 530/30). Best curve fit for Lineweaver−Burk plots and K_i values were determined by using the curve-fitting programs Prism 3.0 (GraphPad Software, Inc., San Diego, CA) and SigmaPlot 2000 Enzyme Kinetics (SSPS Science, Richmond, CA).

Antiproliferative and Chemical Complementation Assays. The proliferation of human MCF-7 breast cancer cells was measured by a previously described colorimetric assay.[34] Briefly, we seeded 2000−4000 cells per well in microtiter plates and allowed them to attach overnight. Cells were then treated with vehicle or compound continuously or for 3 h. After a 48-h incubation in 5% CO_2 atmosphere and 100% humidity, the medium was replaced with serum-free medium containing 0.1% 3-(4,5-dimethylthiazol-2-yl)-2,5-diphenyltetrazolium bromide. Plates were incubated for an additional 3 h in the dark, and the total cell number was determined spectrophotometrically at 540 nm as previously described.[34]

For the chemical complementation assay, HeLa cells were obtained from ATCC and were maintained in Dulbecco's minimum essential medium (DMEM) containing 10% fetal bovine serum (FBS, HyClone, Logan, UT) and 1% penicillin−streptomycin (Life Technologies, Inc., Rockville, MD) in a humidified atmosphere of 5% CO_2 at 37 °C. We used a mammalian expression plasmid encoding full-length wild-type Cdc25A in a pcDNA3 vector generously provided by Thomas Roberts (Dana Farber Cancer Institute, Boston, MA)[3] as previously described.[20]

Acknowledgment. This work was supported by the U.S. Department of Defense, the Fiske Drug Discovery Fund, and the National Institutes of Health. We thank Daniel Zaharevitz and Jill Johnson of the NCI for providing compounds and advice.

Supporting Information Available: HPLC analysis results for DA compounds (with HRMS data). This material is available free of charge via the Internet http://pubs.acs.org.

References

(1) Denu, J. M.; Stuckey, J. A.; Saper, M. A.; Dixon, J. E. Form and function in protein dephosphorylation. *Cell* **1996**, *87*, 361−364.
(2) Nilsson, I.; Hoffmann, I. Cell cycle regulation by the Cdc25 phosphatase family. *Prog. Cell Cycle Res.* **2000**, *4*, 107−114.
(3) Xia, K.; Lee, R. S.; Narsimhan, R. P.; Mukhopadhyay, N. K.; Neel, B. G.; Roberts, T. M. Tyrosine phosphorylation of the proto-oncoprotein Raf-1 is regulated by Raf-1 itself and the phosphatase Cdc25A. *Mol. Cell. Biol.* **1999**, *19*, 4819−4824.
(4) Galaktionov, K.; Beach, D. CDC25 phosphatases as potential human oncogenes. *Cell* **1991**, *67*, 1181−1194.
(5) Sadhu, K.; Reed, S. I.; Richardson, H.; Russell, P. Human homolog of fission yeast Cdc25 mitotic inducer is predominantly expressed in G2. *Proc. Natl. Acad. Sci. U.S.A.* **1990**, *87*, 5139−5143.
(6) Nagata, A.; Igarashi, M.; Jinno, S.; Suto, K.; Okayama, H. An additional homolog of the fission yeast cdc25+ gene occurs in humans and is highly expressed in some cancer cells. *New Biol.* **1991**, *3*, 959−968.
(7) Galaktionov, K.; Lee, A. K.; Eckstein, J.; Draetta, G.; Meckler, J.; Loda, M.; Beach, D. CDC25 phosphatases as potential human oncogenes. *Science* **1995**, *269*, 1575−1577.
(8) Galaktionov, K.; Chen, X.; Beach, D. Cdc25 cell-cycle phosphatase as a target of c-myc. *Nature* **1996**, *382*, 511−517.
(9) Wu, W.; Fan, Y.-H.; Kemp, B. L.; Walsh, G.; Mao, L. Overexpression of *cdc*25A and *cdc*25B is frequent in primary non-small cell lung cancer but is not associated with overexpression of c-*myc*. *Cancer Res.* **1998**, *58*, 4082−4085.
(10) Giulia Cangi, M.; Cukor, B.; Soung, P.; Signoretti, S.; Moreira, J., G.; Ranashinge, M.; Cady, B.; Pagano, M.; Loda, M. Role of the Cdc25A phosphatase in human breast cancer. *J. Clin. Invest.* **2000**, *106*, 753−761.
(11) Millar, J. B.; Blevitt, J.; Gerace, L.; Sadhu, K.; Featherstone, C.; Russell, P. p55CDC25 is a nuclear protein required for the initiation of mitosis in human cells. *Proc. Natl. Acad. Sci. U.S.A.* **1991**, *88*, 10500−10504.
(12) Hoffman, I.; Draetta, G.; Karsenti, E. Activation of the phosphatase activity of human cdc25A by a cdk2-cyclin E dependent phosphorylation at the G1/S transition. *EMBO J.* **1994**, *13*, 4302−4310.
(13) Jinno, S.; Suto, J.; Nagata, A.; Igarashi, M.; Kanaoka, Y.; Nojima, H.; Okayama, H. Cdc25A is a novel phosphatase functioning early in the cell cycle. *EMBO J.* **1994**, *13*, 1549−1556.
(14) Molinari, M.; Mercurilo, C.; Dominguez, J.; Goubin, F.; Draetta, G. F. Human Cdc25 A inactivation is response to S phase inhibition and its role in preventing premature mitosis. *EMBO Rep.* **2000**, *1*, 71−79.
(15) Mailand, N.; Falck, J.; Lukas, C.; Syljuasen, R. G.; Welcker, M.; Lukas, J. Rapid destruction of human Cdc25A in response to DNA damage. *Science* **2000**, *288*, 1425−1429.
(16) Fauman, E. B.; Cogswell, J. P.; Lovejoy, B.; Rocque, W. J.; Holmes, W.; Montana, V. G.; Piwnica-Worms, H.; Rink, M. J.; Saper, M. A. Crystal structure of the catalytic domain of the human cell cycle control phosphatase, Cdc25A. *Cell* **1998**, *93*, 617−625.
(17) Reynolds, R. A.; Yem, A. W.; Wolfe, C. L.; Deibel, J. M. R.; Chidester, C. G.; Watenpaugh, K. D. Crystal structure of the catalytic subunit of Cdc25B required for G2.M phase transition of the cell cycle. *J. Mol. Biol.* **1999**, *293*, 559−568.

(18) Rudolph, J.; Epstein, D. M.; Parker, L.; Eckstein, J. Specificity of natural and artificial substrates for human Cdc25A. *Anal. Biochem*. **2001**, *289*, 43−51.
(19) Chen, W.; Wilborn, M.; Rudolph, J. Dual-specific Cdc25B phosphatase in search of the catalytic acid. *Biochemistry* **2000**, *39*, 10781−10789.
(20) Vogt, A.; Adachi, T.; Ducruet, A. P.; Chesebrough, J.; Nemoto, K.; Carr, B. I.; Lazo, J. S. Spatial analysis of key signaling proteins by high-content solid-phase cytometry in Hep3B cells treated with an inhibitor of Cdc25 dual specificity phosphatases. *J. Biol. Chem*. **2001**, *276*, 20544−20550.
(21) Gunasekera, S. P.; McCarthy, P. J.; Kelly-Borges, M. Dysidiolide: A novel protein phosphatase inhibitor from the Caribbean sponse dysidea etheria de laubenfels. *J. Am. Chem. Soc*. **1996**, *118*, 8759−8760.
(22) Cebula, R. E.; Blanchard, J. L.; Boisclair, M. D.; Pal, K.; Bockovich, N. J. Synthesis and phosphatase inhibitory activity of analogs of sulfircin. *Bioorg. Med. Chem. Lett*. **1997**, *7*, 2015−2020.
(23) Rice, R. L.; Rusnak, J. M.; Yokokawa, F.; Yokokawa, S.; Messner, D. J.; Boynton, A. L.; Wipf, P.; Lazo, J. S. A targeted library of small molecule, tyrosine and dual specificity phosphatase inhibitors derived from a rational core design and random side chain variation. *Biochemistry* **1997**, *36*, 15965−15974.
(24) Ducruet, A. P.; Rice, R. L.; Tamura, K.; Yokokawa, F.; Yokokawa, S.; Wipf, P.; Lazo, J. S. Identification of new Cdc25 dual specificity phosphatase inhibitors in a targeted small molecule array. *Bioorg. Med. Chem*. **2000**, *8*, 1451−1466.
(25) Peng, H.; Xie, W.; Otterness, D. M.; Cogswell, J. P.; McConnell, R. T.; Carter, H. L.; Powis, G.; Abraham, R. T.; Zalkow, L. H. Synthesis and biological activities of a novel group of steroidal derived inhibitors for human Cdc25A protein phosphatase. *J. Med. Chem*. **2001**, *44*, 834−848.
(26) Tamura, K.; Southwick, E. C.; Kerns, J.; Rosi, K.; Carr, B. I.; Wilcox, C.; Lazo, J. S. Cdc25 inhibition and cell cycle arrest by a synthetic thioalkyl vitamin K analogue. *Cancer Res*. **2000**, *60*, 1317−1325.
(27) Fritzen, E. L.; Brightwell, A. S.; Erickson, L. A.; Romero, D. L. The solid phase synthesis of tetrahydroisoquinolines having Cdc25B inhibitory activity. *Bioorg. Med. Chem. Lett*. **2000**, 649−652.
(28) Behforouz, M.; Haddad, J.; Cai, W.; Gu, Z. Chemistry of quinoline-5,8-diones. *J. Org. Chem*. **1998**, 63, 343−346.
(29) Boger, D. L.; Yasuda, M.; Mitscher, L. A.; Drake, S. D.; Kitos, P. A.; Thompson, S. C. Streptonigrin and lavendamycin partial structures. Probes for the minimal, potent pharmacophore of streptonigrin, lavendamycin, and synthetic quinoline-5,8-diones. *J. Med. Chem*. **1987**, *30*, 1918−1928.
(30) Ryu, C.-K.; Lee, I.-K.; Jung, S.-H.; Lee, C.-O. Synthesis and cytotoxicity of 6-chloro-7-arylamino-5,8-isoquinolinediones. *Bioorg. Med. Chem. Lett*. **1999**, *9*, 1075−1080.
(31) Cameron, D. W.; Deutscher, K. R.; Feutrill, G. I. Nucleophilic alkenes. IX. Addition of 1,1-dimethoxyethene to azanaphthoquinones: Synthesis of bostrycoidin and 8-*O*-methylbostrycoidin. *Aust. J. Chem*. **1982**, *35*, 1439−1450.
(32) Yoon, E. Y.; Choi, H. Y.; Shin, K. J.; Yoo, K. H.; Chi, D. Y.; Kim, D. J. The regioselectivity in the reaction of 6,7-dihaloquinoline-5,8-diones with amine nucleophiles in various solvents. *Tetrahedron Lett*. **2000**, *41*, 7475−7480.
(33) Shaikh, I. A.; Johnson, F.; Grollman, A. P. Streptonigrin. 1. Structure−activity relationships among simple bicyclic analogues. Rate dependence of DNA degradation on quinone reduction potential. *J. Med. Chem*. **1986**, *29*, 1329−1340.
(34) Vogt, A.; Rice, R. L.; Settineri, C. E.; Yokokawa, F.; Yokokawa, S.; Wipf, P.; Lazo, J. S. Disruption of insulin-like growth factor-1 signaling and down-regulation of Cdc2 by SC-ααδ9, a novel small molecule antisignaling agent identified in a targeted array library. *J. Pharmacol. Exp. Therap*. **1998**, *287*, 806−813.

JM0102046